

Isoscalar giant monopole resonance for drip-line and super heavy nuclei in the framework of a relativistic mean field formalism with scaling calculation

Editorial

S. K. Biswal* S. K. Patra

Institute Of Physics,
Sachivalya Marg, 751 005, India.

Abstract:

We study the isoscalar giant monopole resonance for drip-lines and super heavy nuclei in the frame work of a relativistic mean field theory with scaling approach. The well known extended Thomas-Fermi approximation in the non-linear σ - ω model is used to estimate the giant monopole excitation energy for some selected light spherical nuclei starting from the region of proton to neutron drip-lines. The application is extended to super heavy region for $Z=114$ and 120 , which are predicted by several models as the next proton magic number beyond $Z=82$. We compared the excitation energy obtained by four successful force parameters NL1, NL3, NL3* and FSUGold. The monopole energy decreases toward the proton and neutron drip-lines in an isotopic chain for lighter mass nuclei contrary to a monotonous decrease for super heavy isotopes. The maximum and minimum monopole excitation energies are obtained for nuclei with minimum and maximum isospin, respectively in an isotopic chain.

PACS (2008): 21.10.Dr, 21.65.Cd, 21.60.-n, 21.10.-k

Keywords: Relativistic Thomas-Fermi approximation, Monopole excitation energy, Compressibility modulus

© Versita sp. z o.o.

1. Introduction

The study of nuclei far away from the drip-lines has a current research interest due to their very different properties than the nuclei at the β -stability valley. New properties of these nuclei like the soft giant resonance, the change of magic number, the halo and skin structures and the new decay modes stimulate strongly the research using radioactive ion beam (RIB) [1, 2]. On the other hand, the super heavy nuclei which are on the stability line, but extremely unstable due to the excessive Coulomb repulsion attract much theoretical attention for its resemblance to the highly asymmetry nuclear matter limit [3, 4]. These nuclei possess a large amount of collective excitation and their study along an isotopic chain is more informative for the structural evaluation of astrophysical objects

* E-mail: sbiswal@iopb.res.in

like neutron star [5]. Also, the nuclear symmetry energy, and consequently the proton to neutron ratio, are crucial factors in constructing the equation of state (EOS) for asymmetry nuclear matter.

The compressibility K_A of a nuclear system depends on its neutron-proton asymmetry. Also it is well known that the EOS of an asymmetry accerating object like neutron star substantially influence by it's compressibility. Although, the compressibility at various asymmetry is an important quantities, it is not a direct experimental observable. Thus, one has to determine the K_A from the linked experimental quantity (which is directly or indirectly related to K_A) like isoscalar giant monopole resonance (ISGMR) [6, 7]. The ISGMR is a well defined experimental observable, which can be measured precisely through various experimental techniques. The drip-lines and super heavy nuclei are vulnerable and unstable in nature because of the presence of excess neutron and large number of protons, respectively. Thus it is instructive to know the giant monopole resonance, compressibility modulus and other related quantities for both drip-lines and super heavy nuclei. In this context, our aim is to study the giant monopole excitation energy and the compressional modulus of finite nuclei near the drip-line [2] as well as for recently discussed super heavy nuclei with proton numbers $Z=114$ and 120 , which are predicted to be next magic numbers beyond $Z=82$ with various models [8, 9]. In addition, the calculations of Refs. [10, 11] suggest that these nuclei possess spherical ground state or low-lying spherical excited solutions. More specifically, we aimed to study the following within the frame-work of an extended relativistic Thomas-Fermi approximation:

- How the isoscalar excitation energy and the finite nuclear compressibility varies in an isotopic chain in drip-lines and super heavy nuclei within a well tested model like relativistic extended Thomas-Fermi frame work using scaling and constrained approaches which is developed by some of us recently [12, 13].
- A comparative study of ISGMR obtained with various parameter sets such as NL1, NL3, NL3* and FSUGold for the same drip-lines and super heavy nuclei.
- The resonance width Σ , which is mostly the difference between the scaling and constraint excitation energies are analyzed in the isotopic chains of light and super heavy nuclei.
- Finally, the relation between the finite nuclear compressibility with the infinite nuclear matter values in various force parameter sets are looked for.

In relativistic mean field (RMF) formalism the NL1 parameter set [14] is considered to be one of the best interaction for a long time to predict the experimental observables. The excessive large value of asymmetry coefficient $J \sim 43.6$ MeV questions about the accuracy for the prediction of neutron radius near the drip-line. As a result, the discovery of NL3 parameter set [16] complement the limitation of NL1 force and evaluates the ground state properties of finite nuclei in an excellent agreement with experiment [15–20]. It reproduces the proton or charge radius r_c precisely along with the ground state binding energy. Unfortunately, the experimental data for neutron radius has a large error bar [21], which covers most of the prediction of all relativistic and non-relativistic models [22]. The FSUGold parameter set [23, 24] reproduces the ISGMR pretty well with the experimental data

for ^{90}Zr and ^{208}Pb . There is also a possibility to solve the uncertainty in neutron radius problem [25] using this interaction. The NL3* force parametrization [26] claimed to be an improved version of NL3 to reproduce the experimental observables. We used all these forces and made a comparison of their predictive power for various experimental data. Then we selected NL3 as a suitable parameter set for our further investigations for ISGMR and related quantities.

The paper is presented as follows: In section II, we outline in brief the formalism used in the present work. In section III, we discuss our results for the ground state isoscalar giant monopole resonance (ISGMR) for drip-lines and super heavy nuclei. The isoscalar monopole excitation energy E_x and the compressibility modulus of finite nuclei K_A are also analyzed. We give the summary and concluding remarks in section IV.

2. The Formalism

In this paper we shall make use of the principle of scale invariance to obtain the virial theorem for the relativistic mean field [27] theory by working in the relativistic Thomas–Fermi (RTF) and relativistic extended Thomas–Fermi (RETF) approximations [12, 28–32]. Although, the scaling and constrained calculations are not new, the present technique is developed first time by Patra et al [12, 33] and not much have been explored for various regions of the periodic chart. Thus, it is interesting to apply the model specially for drip-lines and super heavy nuclei. The calculations will be explored to the region ranging from $Z=8$ to $Z=114$, 120, where we can simulate the properties of neutron matter from the neutron-rich finite nuclei. For this purpose we compute moments and average centroid energies of the isoscalar giant monopole resonance (ISGMR) through scaling and constrained self-consistent calculations for ground state.

The detail formalisms of the scaling method are given in Refs. [12, 13]. For completeness, we have outlined briefly some of the essential expressions which are needed for the present purpose. We have worked with the non-linear Lagrangian of Boguta and Bodmer [34] to include the many-body correlation arises from the non-linear terms of the σ -meson self-interaction [35] for nuclear many-body system. The nuclear matter compressibility modulus K_∞ also reduces dramatically by the introduction of these terms, which motivates to work with this non-linear Lagrangian. The relativistic mean field Hamiltonian for a nucleon-meson interacting system is written by [12, 27]:

$$\begin{aligned} \mathcal{H} = & \sum_i \varphi_i^\dagger \left[-i\vec{\alpha} \cdot \vec{\nabla} + \beta m^* + g_v V + \frac{1}{2} g_\rho R \tau_3 \right. \\ & + \left. \frac{1}{2} e\mathcal{A}(1 + \tau_3) \right] \varphi_i + \frac{1}{2} \left[(\vec{\nabla}\phi)^2 + m_s^2 \phi^2 \right] + \frac{1}{3} b\phi^3 \\ & + \frac{1}{4} c\phi^4 - \frac{1}{2} \left[(\vec{\nabla}V)^2 + m_v^2 V^2 \right] \\ & - \frac{1}{2} \left[(\vec{\nabla}R)^2 + m_\rho^2 R^2 \right] - \frac{1}{2} \left(\vec{\nabla}\mathcal{A} \right)^2. \end{aligned} \quad (1)$$

Here m , m_s , m_v and m_ρ are the masses for the nucleon (with $m^* = m - g_s\phi$ being the effective mass of the nucleon), σ -, ω - and ρ -mesons, respectively and φ is the Dirac spinor. The field for the σ -meson is denoted

by ϕ , for ω -meson by V , for ρ -meson by R (τ_3 as the 3rd component of the isospin) and for photon by A . g_s , g_v , g_ρ and $e^2/4\pi=1/137$ are the coupling constants for the σ , ω , ρ -mesons and photon respectively. b and c are the non-linear coupling constants for σ mesons. By using the classical variational principle we obtain the field equations for the nucleon and mesons. In semi-classical approximation we can write the above Hamiltonian in term of density as:

$$\mathcal{H} = \mathcal{E} + g_v V \rho + g_\rho R \rho_3 + e \mathcal{A} \rho_p + \mathcal{H}_f, \quad (2)$$

where

$$\mathcal{E} = \sum_i \varphi_i^\dagger \left[-i \vec{\alpha} \cdot \vec{\nabla} + \beta m^* \right] \varphi_i, \quad (3)$$

$$\rho_s = \sum_i \varphi_i^\dagger \varphi_i, \quad (4)$$

$$\rho = \sum_i \bar{\varphi}_i \varphi_i, \quad (5)$$

$$\rho_3 = \frac{1}{2} \sum_i \varphi_i^\dagger \tau_3 \varphi_i, \quad (6)$$

and \mathcal{H}_f is the free part of the Hamiltonian. The total density ρ is the sum of proton ρ_p and neutron ρ_n densities. The semi-classical ground-state meson fields are obtained by solving the Euler–Lagrange equations $\delta \mathcal{H} / \delta \rho_q = \mu_q$ ($q = n, p$).

$$(\Delta - m_s^2) \phi = -g_s \rho_s + b \phi^2 + c \phi^3, \quad (7)$$

$$(\Delta - m_v^2) V = -g_v \rho, \quad (8)$$

$$(\Delta - m_\rho^2) R = -g_\rho \rho_3, \quad (9)$$

$$\Delta \mathcal{A} = -e \rho_p. \quad (10)$$

The above field equations are solved self-consistently in an iterative method. The pairing correlation is not included in the evaluation of the equilibrium property as well as monopole excitation energy. The Thomas-Fermi approach is a semi-classical approximation and pairing correlation has a minor role in giant resonance. It is shown in [36, 37] that only for open-shell nuclei, it has a marginal effect on ISGMR energy. As far as pairing correlation is concerned, it is a quantal effect and can be included in a semi classical calculation as an average as it is adopted in semi-empirical mass formula. In Ref. [36], perturbative calculation on top of a semi classical approach is done,

and it suggests that pairing correlation is unimportant in such approach like relativistic Thomas-Fermi (RTF) or relativistic extended Thomas-Fermi (RETF) approximations. In our present calculations, the scalar density (ρ_s) and energy density (\mathcal{E}) are calculated using RTF and RETF formalisms. The RETF is the \hbar^2 correction to the RTF, where the gradient of density is taken care. This term of the density takes care of the variation of the density and involves more in the surface properties.

$$\mathcal{H} = \mathcal{E} + \frac{1}{2}g_s\phi\rho_s^{eff} + \frac{1}{3}b\phi^3 + \frac{1}{4}c\phi^4 + \frac{1}{2}g_vV\rho + \frac{1}{2}g_\rho R\rho_3 + \frac{1}{2}e\mathcal{A}\rho_p, \quad (11)$$

with

$$\rho_s^{eff} = g_s\rho_s - b\phi^2 - c\phi^3. \quad (12)$$

In order to study the monopole vibration of the nucleus we have scaled the baryon density [12]. The normalized form of the baryon density is given by

$$\rho_\lambda(\mathbf{r}) = \lambda^3\rho(\lambda r), \quad (13)$$

λ is the collective co-ordinate associated with the monopole vibration. As Fermi momentum and density are inter-related, the scaled Fermi momentum is given by

$$K_F q \lambda = [3\pi^2\rho_q\lambda(\mathbf{r})]^{1/3}. \quad (14)$$

Similarly ϕ , V , R and Coulomb fields are scaled due to self-consistence eqs. (7-10). But the ϕ field can not be scaled simply like the density and momentum, because the source term of ϕ field contains the ϕ field itself. In semi-classical formalism, the energy and density are scaled like

$$\begin{aligned} \mathcal{E}_\lambda(\mathbf{r}) &= \lambda^4\tilde{\mathcal{E}}(\lambda\mathbf{r}) \\ &= \lambda^4[\tilde{\mathcal{E}}_0(\lambda\mathbf{r}) + \tilde{\mathcal{E}}_2(\lambda\mathbf{r})], \end{aligned} \quad (15)$$

$$\rho_{s\lambda}(\mathbf{r}) = \lambda^3\tilde{\rho}_s(\lambda\mathbf{r}). \quad (16)$$

The symbol \sim shows an implicit dependence of \tilde{m}^* . With all these scaled variables, we can write the Hamiltonian as:

$$\begin{aligned} \mathcal{H}_\lambda &= \lambda^3\lambda\tilde{\mathcal{E}} + \frac{1}{2}g_s\phi_\lambda\tilde{\rho}_s^{eff} + \frac{1}{3}\frac{b}{\lambda^3}\phi_\lambda^3 + \frac{1}{4}\frac{c}{\lambda^3}\phi_\lambda^4 \\ &+ \frac{1}{2}g_vV_\lambda\rho + \frac{1}{2}g_\rho R_\lambda\rho_3 + \frac{1}{2}eA_\lambda\rho_p. \end{aligned} \quad (17)$$

Here we are interested to calculate the monopole excitation energy which is defined as $E^s = \sqrt{\frac{C_m}{B_m}}$ with C_m is the restoring force and B_m is the mass parameter. In our calculations, C_m is obtained from the double derivative of the scaled energy with respect to the scaled co-ordinate λ at $\lambda = 1$ and is defined as [12]:

$$C_m = \int dr \left[-m \frac{\partial \tilde{\rho}_s}{\partial \lambda} + 3 \left(m_s^2 \phi^2 + \frac{1}{3} b \phi^3 - m_v^2 V^2 - m_\rho^2 R^2 \right) - (2m_s^2 \phi + b \phi^2) \frac{\partial \phi_\lambda}{\partial \lambda} + 2m_v^2 V \frac{\partial V_\lambda}{\partial \lambda} + 2m_\rho^2 R \frac{\partial R_\lambda}{\partial \lambda} \right]_{\lambda=1}, \quad (18)$$

and the mass parameter B_m of the monopole vibration can be expressed as the double derivative of the scaled energy with the collective velocity $\dot{\lambda}$ as

$$B_m = \int dr U(\mathbf{r})^2 \mathcal{H}, \quad (19)$$

where $U(\mathbf{r})$ is the displacement field, which can be determined from the relation between collective velocity $\dot{\lambda}$ and velocity of the moving frame,

$$U(\mathbf{r}) = \frac{\mathbf{1}}{\rho(\mathbf{r})\mathbf{r}^2} \int d\mathbf{r}' \rho_T(\mathbf{r}') \mathbf{r}'^2, \quad (20)$$

with ρ_T is the transition density defined as

$$\rho_T(\mathbf{r}) = \left. \frac{\partial \rho_\lambda(\mathbf{r})}{\partial \lambda} \right|_{\lambda=1} = 3\rho(\mathbf{r}) + \mathbf{r} \frac{\partial \rho(\mathbf{r})}{\partial \mathbf{r}}, \quad (21)$$

taking $U(\mathbf{r}) = \mathbf{r}$. Then the mass parameter can be written as $B_m = \int dr r^2 \mathcal{H}$. In non-relativistic limit, $B_m^{nr} = \int dr r^2 m \rho$ and the scaled energy E_m^s is $\sqrt{\frac{m_3}{m_1}}$. The expressions for m_3 and m_1 can be found in [7]. Along with the scaling calculation, the monopole vibration can also be studied with constrained approach [7, 38–41]. In this method, one has to solve the constrained functional equation:

$$\int dr [\mathcal{H} - \eta r^2 \rho] = E(\eta) - \eta \int dr r^2 \rho. \quad (22)$$

Here the constrained is $\langle R^2 \rangle_0 = \langle r^2 \rangle_m$. The constrained energy $E(\eta)$ can be expanded in a harmonic approximation as

$$E(\eta) = E(0) + \left. \frac{\partial E(\eta)}{\partial \eta} \right|_{\eta=0} + \left. \frac{\partial^2 E(\eta)}{\partial \eta^2} \right|_{\eta=0}. \quad (23)$$

The second order derivative in the expansion is related with the constrained compressibility modulus for finite nucleus K_A^c as

$$K_A^c = \frac{1}{A} R_0^2 \frac{\partial^2 E \eta}{\partial R_\eta}, \quad (24)$$

and the constrained energy E_m^c as

$$E_m^c = \sqrt{\frac{AK_m^c}{B_m^c}}. \quad (25)$$

In the non-relativistic approach, the constrained energy is related by the sum rule weighted $E_m^c = \sqrt{\frac{m_1}{m_{-1}}}$. Now the scaling and constrained excitation energies of the monopole vibration in terms of the non-relativistic sum rules will help us to calculate Σ , i.e., the resonance width [7, 42],

$$\Sigma = \sqrt{(E_m^s)^2 - (E_m^c)^2} = \sqrt{\left(\frac{m_3}{m_1}\right)^2 - \left(\frac{m_1}{m_{-1}}\right)^2}. \quad (26)$$

3. Results and Discussions

3.1. Force parameter of relativistic mean field formalism

First of all, we examined the predictive power of various parameter sets. In this context we selected NL1 as a successful set of past and few recently used forces like NL3, NL3* and FSUGold. The ground state observables obtained by these forces are depicted in Table 1. Along with the relativistic extended Thomas-Fermi (RETF) results, the values with relativistic Hartree are also compared with the experimental data [43, 44]. The calculated RMF results obtained by all the force parameters considered in the present paper are very close to the experimental data [43, 44]. A detail analysis of the binding energy and charge radius clear that NL1 and FSUGold have a superior predictive power for ^{16}O in RMF level. The advantage of FSUGold decreases with increase of mass number of the nucleus. Although, the predictive power of the pretty old NL1 set is very good for binding energy, it has a large asymmetry coefficient J , which may mislead the prediction in unknown territory, like neutron drip-line or super heavy regions. The RETF prediction of binding energy and charge radius (numbers in the parenthesis) is very poor with the experimental data as compared to the RMF calculations. However, for relatively heavier masses, the ERTF results can be used within acceptable error. In general, taking into account the binding energy BE and root mean square charge radius r_c , one may prefer to use either NL3 or NL3* parametrization. Before accepting NL3 or NL3* as the usable parameter set for our further calculations, in Table 2, we have given the excitation energy of some selective nuclei both in light and super heavy regions with various parameter sets for some further verification. The isoscalar giant monopole energies E^s and E^c are evaluated using both scaling and constraint calculations, respectively. The forces like NL1, NL3, NL3* and FSUG have a wide range of compressibility K_∞ starting from 211.7 to 271.7 MeV (see Table 1). Because of the large variation in K_∞ of these sets, we expect various values of E^s and E^c with different parametrization. From Table 2, it is noticed that the calculated results for ^{16}O and ^{40}Ca differ substantially from the data. Again this deviation of calculated result goes on decreasing with increase of mass number, irrespective of the parameter set. This may be due to the use of semi-classical approximation like Thomas-Fermi and extended Thomas-Fermi. In these approaches, quantal corrections are averaged out. When we are going from light to the heavy and then super

Table 1. The calculated binding BE and charge radius r_c obtained from relativistic extended Thomas-Fermi (RETF) approximation is compared with relativistic Hartree (with various parameter sets) and experimental results [43, 44]. The RETF results are given in the parenthesis. The empirical values [45, 46] of nuclear matter saturation density ρ_0 , binding energy per nucleon BE/A, compressibility modulus K , asymmetry parameter J and ratio of effective mass to the nucleon mass M^*/M are given in the lower part of the table. The energy is in MeV and radius is in fm.

Nucleus	Set	BE (calc.)	BE (Expt.)	r_c (calc.)	r_c (Expt.)
^{16}O	NL1	127.2(118.7)	127.6	2.772(2.636)	2.699
	NL3	128.7(120.8)		2.718(2.591)	
	NL3*	128.1(119.5)		2.724(2.603)	
	FSUG	127.4(117.8)		2.674(2.572)	
^{40}Ca	NL1	342.3(344.783)	342.0	3.501(3.371)	3.478
	NL3	341.6(346.2)		3.470(3.343)	
	NL3*	341.5(344.2)		3.470(3.349)	
	FSUG	340.8(342.2)		3.429(3.327)	
^{48}Ca	NL1	412.7(419.5)	416.0	3.501(3.445)	3.477
	NL3	414.6(422.6)		3.472(3.426)	
	NL3*	413.5(420.3)		3.469(3.429)	
	FSUG	411.2(418.0)		3.456(3.418)	
^{90}Zr	NL1	784.3(801.1)	783.9	4.284(4.232)	4.269
	NL3	781.4(801.7)		4.273(4.219)	
	NL3*	781.6(798.7)		4.267(4.219)	
	FSUG	778.8(797.3)		4.257(4.214)	
^{116}Sn	NL1	989.5(1013.7)	988.7	4.625(4.583)	4.625
	NL3	985.4(1014.6)		4.617(4.571)	
	NL3*	986.4(1011.0)		4.609(4.569)	
	FSUG	984.4(1010.7)		4.611(4.569)	
^{208}Pb	NL1	1638.1(1653.7)	1636.4	5.536(5.564)	5.501
	NL3	1636.9(1661.2)		5.522(5.541)	
	NL3*	1636.5(1655.2)		5.512(5.538)	
	FSUG	1636.2(1661.4)		5.532(5.541)	
Set	NL1	NL3	NL3*	FSUG	empirical
ρ_0	0.154	0.150	0.148	0.148	0.17
E/A	16.43	16.31	16.30	16.30	15.68
K	211.7	271.76	258.27	230.0	210 ± 30
J	43.6	38.68	37.4	32.597	32 ± 2
M^*/M	0.57	0.594	0.60	0.61	0.6

heavy nuclei, the surface correction decreases appreciably. Consequently, the contribution to monopole excitation energy decreases with mass number A . In column 11, 12 and 13 of Table 2, the differences in E_x obtained from various parameter sets are given, namely, Δ_1 is the difference in monopole excitation energy obtained by NL3 and NL3*. Similarly, Δ_2 and Δ_3 are the ISGMR difference with (NL3*, FSUG) and (NL3, FSUG), respectively. The values of Δ_1 , Δ_2 or Δ_3 goes on decreasing with increase of mass number of the nucleus without depending on the parameter used. In other word, we may reach to same conclusion in the super heavy region irrespective of the parameter set. However, it is always better to use a successful parameter set to explore an unknown territory. In this context, it is safer to choose NL3 force for our further exploration. The second observation is also apparent from the Table. It is commonly believe that, mostly the compressibility of the force parameter affect the excitation energy of ISGMR of the nucleus. That means force parameters having different K_∞ have

Table 2. The results of isoscalar giant monopole resonance with various parameter sets for some known nuclei are compared with recent experimental data [47]. The calculations are done with relativistic extended Thomas-Fermi (RETF) approximation using both scaling and constrained schemes. The values of Δ_1 , Δ_2 and Δ_3 are obtained by subtracting the results of (NL3, NL3*), (NL3*, FSUG) and (NL3, FSUG), respectively. The monopole excitation energies with scaling E^s and constrained E^c are in MeV.

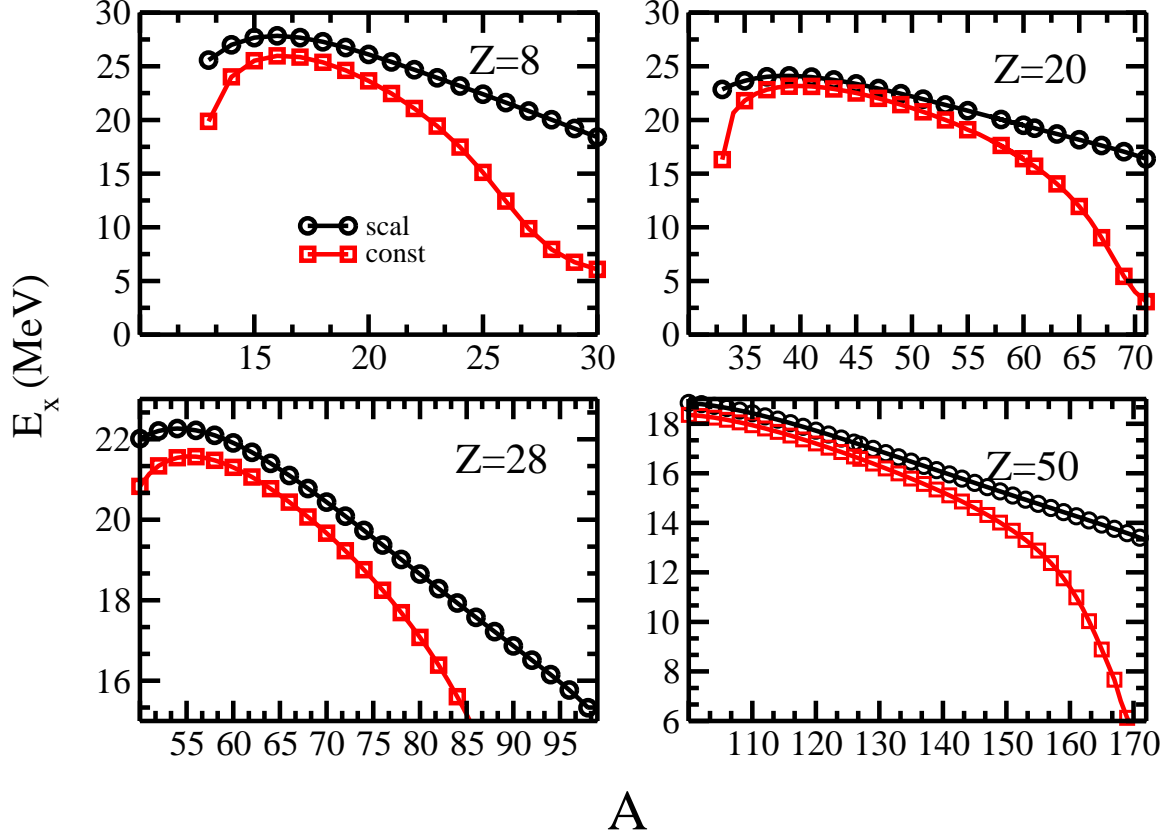
Nucleus	NL1		NL3		NL3*		FSUG		Expt.	Δ_1	Δ_2	Δ_3
	E^s	E^c	E^s	E^c	E^s	E^c	E^s	E^c				
^{16}O	23.31	21.75	27.83	25.97	26.86	25.20	26.97	25.17	21.13±0.49	0.97	0.11	0.86
^{40}Ca	20.61	19.77	24.01	23.16	23.32	22.48	22.98	22.30	19.20±0.40	0.69	0.43	1.03
^{48}Ca	19.51	18.67	22.69	21.73	22.01	21.11	21.72	20.88	19.90±0.20	0.68	0.29	0.97
^{90}Zr	16.91	16.41	19.53	19.03	18.97	18.50	18.60	18.21	17.89 ± 0.20	0.56	0.37	0.97
^{110}Sn	15.97	15.50	18.42	17.94	17.90	17.44	17.52	17.13		0.52	0.38	0.90
^{112}Sn	15.87	15.39	18.29	17.81	17.78	17.32	17.42	17.02	16.1±0.10	0.51	0.36	0.86
^{114}Sn	15.76	15.28	18.16	17.67	17.65	17.18	17.31	16.90	15.9±0.10	0.51	0.34	0.85
^{116}Sn	15.63	15.19	18.02	17.52	17.51	17.04	17.19	16.77	15.80±0.10	0.51	0.32	0.83
^{118}Sn	15.51	15.03	17.87	17.36	17.37	16.89	17.07	16.63	15.6±0.10	0.50	0.30	0.80
^{120}Sn	15.38	14.90	17.72	17.20	17.22	16.73	16.94	16.49	15.4±0.20	0.50	0.28	0.78
^{122}Sn	15.24	14.76	17.56	17.03	17.07	16.57	16.81	16.34	15.0±0.20	0.49	0.24	0.77
^{124}Sn	15.11	14.61	17.40	16.85	16.91	16.40	16.67	16.19	14.80±0.20	0.48	0.24	0.72
^{208}Pb	12.69	12.11	14.58	13.91	14.18	13.55	14.04	13.44	14.17±0.28	0.40	0.14	0.54
$^{286}\text{114}$	11.32	10.60	13.00	12.14	12.64	11.83	12.55	11.79		0.36	0.09	0.45
$^{298}\text{114}$	11.05	10.31	12.68	11.80	12.33	11.50	12.29	11.53		0.35	0.04	0.37
$^{292}\text{120}$	11.28	10.53	12.96	12.07	12.60	11.76	12.48	11.69		0.36	0.12	0.27
$^{304}\text{120}$	11.04	10.28	12.67	11.77	12.33	11.47	12.25	11.47		0.34	0.08	0.42

Table 3. The predicted proton and neutron drip-lines PDL and NDL for O, Ca, Ni, Sn, Pb, Z=114 and Z=120 in relativistic mean field formalism (RMF) with various parameter sets are compared with experimental (where ever available) and Finite Range Droplet Model (FRDM) prediction.

Nucleus	RMF								FRDM		Expt.	
	NL1		NL3		NL3*		FSUG		PDL	NDL	PDL	NDL
	PDL	NDL	PDL	NDL	PDL	NDL	PDL	NDL				
O	12	29	13	30	12	30	12	27	12	26	12	28#
Ca	34	69	33	71	34	71	34	66	30	73	35#	58 #
Ni	49	94	50	98	50	98	51	94	46	99	48	79
Sn	99	165	100	172	100	172	99	1 64	94	169	99#	138#
Pb	178	275	180	281	180	280	179	269	175	273	178	220#
114	267	375	271	392	274	390	271	376	269	339	285#	289#
120	285	376	288	414	288	410	289	396	287	339	-	-

different excitation energy for the same nucleus. For example, ^{208}Pb has excitation energy 14.58 and 14.04 MeV with NL3 and FSUGold, respectively. Although, the ground state binding energy of ^{208}Pb , either with Hartree (RMF) or RETF approximation matches well with NL3 and FSUGold parameter sets (see Table 1), their ISGMR differ by 0.54 MeV, which is quite substantial. This unequal prediction of E^s may be due to the difference in nuclear matter compressibility of the force parametrizations.

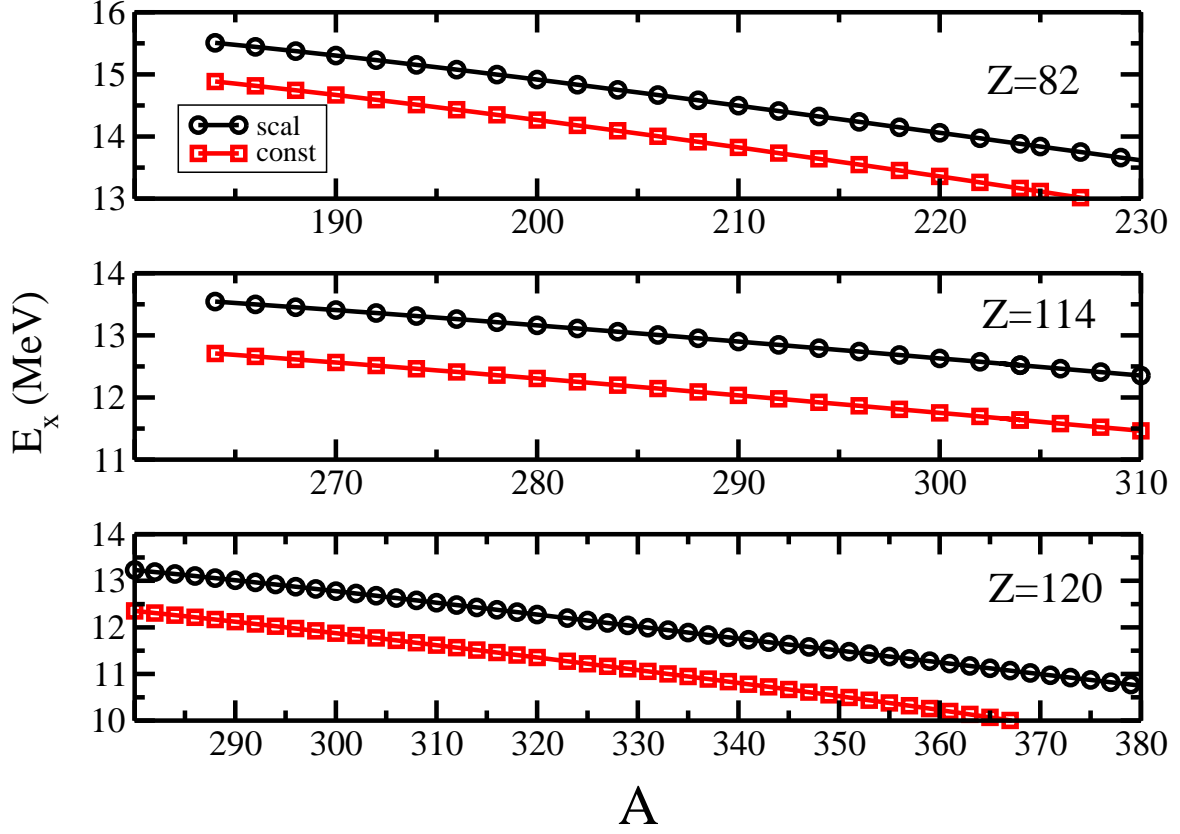
Figure 1. The isoscalar giant monopole resonance (ISGMR) for O, Ca, Ni and Sn isotopes from proton to neutron drip-lines as a function of mass number.



3.2. Proton and neutron drip-lines

In Table 3 we have shown the proton and neutron drip-lines (PDL and NDL) for various parameter sets. The neutron (or proton) drip-line of an isotope is defined when the neutron (or proton) separation energy S_n (or S_p) ≤ 0 , where $S_n = BE(N, Z) - BE(N - 1, Z)$ or $S_p = BE(N, Z) - BE(N, Z - 1)$ with $BE(N, Z)$ is the binding energy of a nucleus with N neutron and Z proton. From the table, it is seen that all the interactions predict almost similar proton and neutron drip-lines. If one compares the drip-lines of NL3 and NL3*, then their predictions are almost identical, explicitly for lighter mass nuclei. Thus, the location of drip-line with various forces does not depend on its nuclear matter compressibility or asymmetry coefficient. For example, the asymmetry coefficient $J = 43.6$ MeV and $K_\infty = 211.7$ MeV for NL1 set and these are 38.68 and 271.76 MeV with NL3 parametrization. The corresponding proton drip-lines for O isotopes are 12 and 13, and the neutron drip-lines are 29 and 30, respectively. The similar effects are noticed for other isotopes of the considered nuclei (see Table 3).

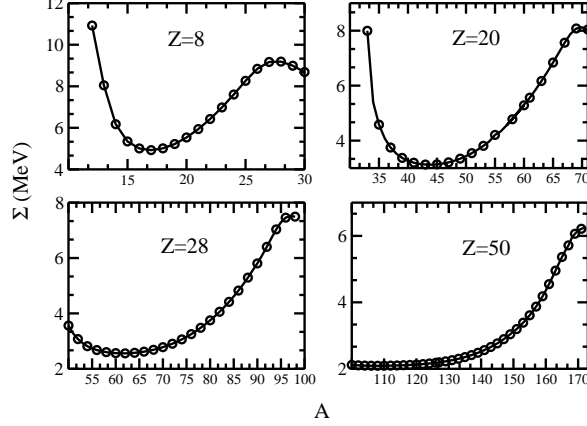
Figure 2. The isoscalar giant monopole resonance (ISGMR) for Pb, Z=114 and Z=120 isotopes starting from proton to neutron drip-lines as a function of mass number.



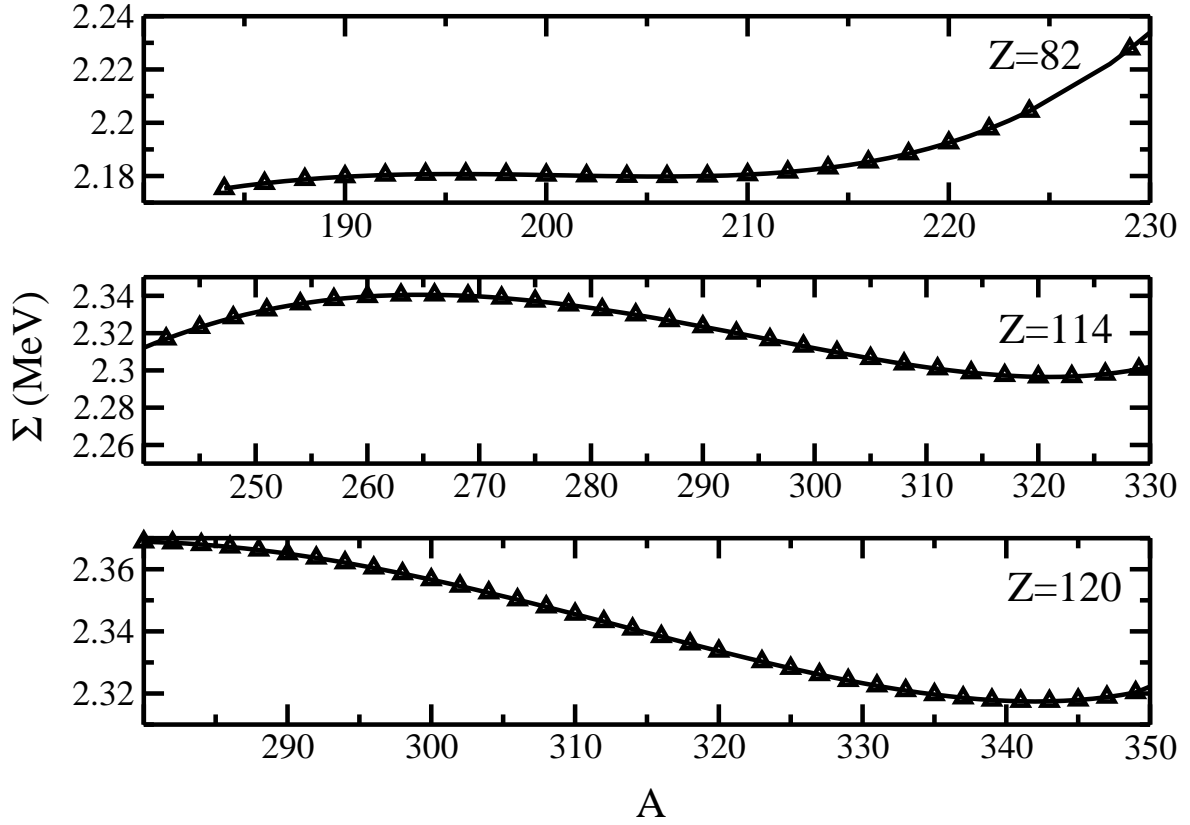
3.3. Isoscalar giant monopole resonance

It is well understood that the isoscalar giant monopole resonance has a direct relation with the compressibility of nuclear matter which decides the softness or stiffness of an equation of state [46]. This EOS also estimates the structure of neutron stars, like mass and radius. Thus, the ISGMR is an intrinsic property of finite nuclei as well as nuclear equation of states and needed to be determined to gain some light for nuclear properties. The ISGMR for O, Ca, Ni, Sn, Pb, Z=114 and Z=120 isotopic series are given in Figs. 1 and 2. The results are calculated by using both constrained and scaling approaches in the isotopic chain, starting from proton to neutron drip-lines. We use the notation $E_m^s = \sqrt{\frac{AK^s}{B_m}}$ with the mass parameter $B_m = \int dr r^2 \mathcal{H}$. The figure shows that excitation energy obtained from scaling calculation is always greater than the constrained value. The difference between the monopole excitation of scaling and constrained calculations, generally gives the resonance width $\Sigma = \frac{1}{2} \sqrt{E_3^2 - E_1^2}$, with $E_3 = \sqrt{\frac{m_3}{m_1}}$ and $E_1 = \sqrt{\frac{m_1}{m_1}}$ in terms of the ratios of the integral moments $m_k = \int_0^\infty d\omega \omega^k S(\omega)$ of the RAP strength function $S(\omega)$ [29]. It is also equivalent to $m_1 = \frac{2}{m} A \langle r^2 \rangle$ and from dielectric theorem, we have $m_{-1} = -\frac{1}{2} A \left(\frac{\partial R_\eta^2}{\partial \eta} \right)_{\eta=0}$.

Figure 3. The difference between the monopole excitation energies of scaling and constrained calculations $\Sigma = \frac{1}{2}\sqrt{E_3^2 - E_1^2}$ as a function of mass number A for O, Ca, Ni and Sn.

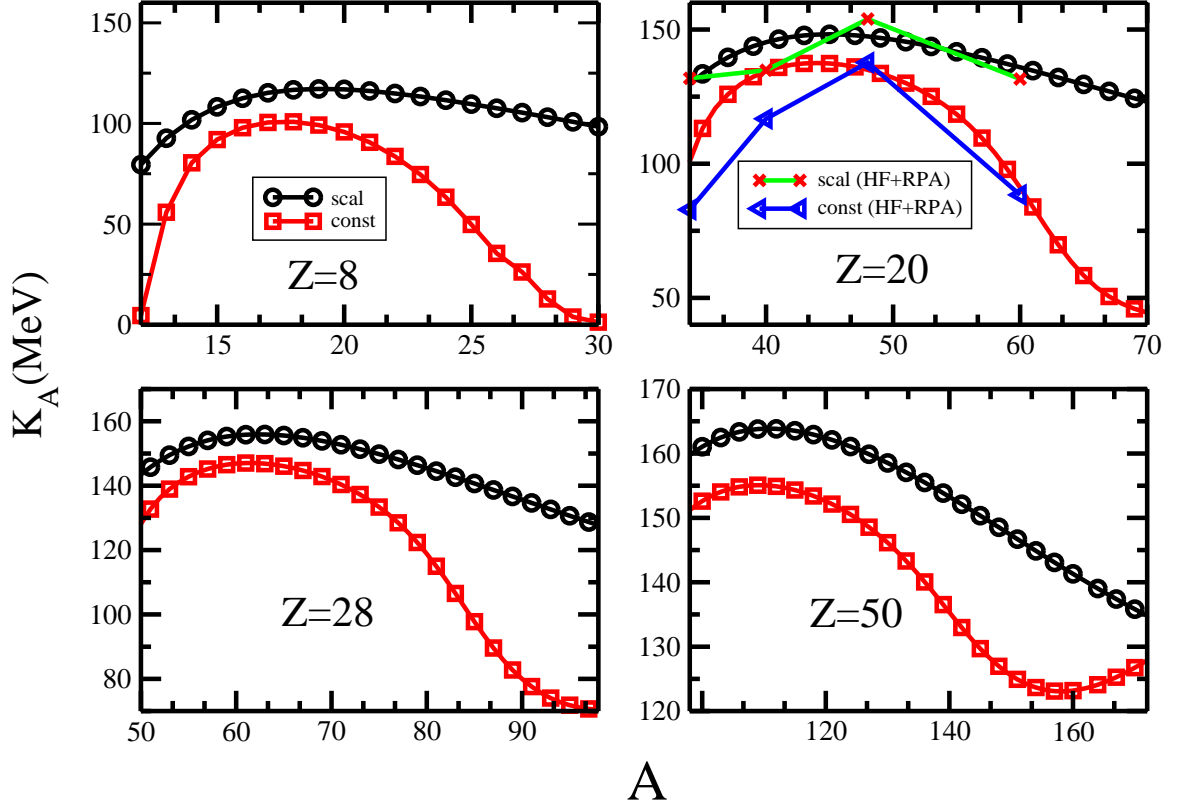


Now consider Fig. 1, where the excitation energy of giant isoscalar monopole resonance E_x for lighter mass nuclei are plotted. For $Z=8$ the excitation energy decreases towards both proton ($A=12$, $E_x^s = 22.51$ MeV) and neutron drip-lines ($A=26$, $E_x^s = 21.22$ MeV). This excitation energy has maximum value near $N=Z$ (here it is a double closed isotope with $Z=8$, $N=8$, $E_x^s = 27.83$ MeV). Similar trends are followed in isotopic chain of Ca with $Z=20$. We find maximum excitation energy at ^{40}Ca ($E_x^s = 24.07$ MeV), whereas E_x^s is found to be smaller both in proton ($A=34$, $E_x = 23.31$ MeV) and neutron drip-lines ($A=71$, $E_x^s = 16.80$ MeV). However, the trends are somewhat different for isotopic chain of higher Z like $Z=50$, 82 , 114 and 120 . In these series of nuclei, the excitation energy monotonically decreases starting from proton drip-line to neutron drip-line. For example, ^{180}Pb and ^{280}Pb are the proton and neutron drip nuclei having excitation energy $E_x = 15.63$ and $E_x = 11.45$ MeV, respectively. Fig. 2 shows clearly the monotonous decrease of excitation energy for super heavy nuclei. This discrepancy between super heavy and light nuclei may be due to Coulomb interaction and large value of isospin difference. For lighter value of Z , the proton drip-line occurs at a combination of proton and neutron where the neutron number is less than or nearer to the proton number. But for higher Z nuclei, the proton drip-line exhibits at a larger isospin. As the excitation energy of a nucleus is a collective property, it varies smoothly with its mass number, which also reflects in the figures. Consider the isotopic chain of $Z=50$, the drip-line nucleus ($A=100$) has excitation energy 18.84 MeV and the neutron drip nucleus $A=171$ has $E_x = 13.39$ MeV. The difference in excitation energy of these two isotopes is 5.32 MeV. This difference in proton and neutron drip nuclei is 4.31 MeV for $Z=82$ and this is 2.37 MeV in $Z=114$. In summary, for higher Z nuclei, the variation of excitation energy in an isotopic chain is less than the lighter Z nucleus. Again, by comparing with the empirical formula of $E_x = CA^{-1/3}$, our predictions show similar variation through out the isotopic chains. Empirically, the value of C is found to be 80 [48], however if we select $C = 70 - 80$ for lighter mass isotopes and $C = 80 - 86$ for super heavy region, then it fits well with our results, which is slightly different than $C=80$ obtained by fitting the data for stable nuclei [48].

Figure 4. Same as Fig. 3, but for Pb, Z=114 and 120.

There is no direct way to calculate Σ in the scaling or constrained method as random phase approximation (RPA). If we compare the excitation energy obtained from scaling calculation with the non-relativistic RPA result, then it is evident that the scaling gives the upper limit of the energy response function. On the other hand, the constrained calculation predicts the lower limit [7]. As a result, the response width Σ is obtained from the root square difference of E_x^s and E_x^c . We have plotted the Σ for the light nuclei in Fig. 3 and for super heavy in Fig. 4. For lighter nuclei, Σ is large both in proton and neutron drip-lines. As one proceed from proton to neutron drip-line, the value of Σ decreases up to a zero isospin combination ($N=Z$ or double close) and then increases. For example, $\Sigma= 10.92, 5.0$ and 21.62 MeV for ^{12}O , ^{16}O and ^{26}O , respectively. Similar trends are also followed by $Z=20, 28$ and 50 isotopic chains. This conclusion can be drawn from the results of the excitation energy also (see Figs. 1 and 2), i.e., the difference between the scaling and constrained excitation energies are more in proton and neutron drip-lines as compared to the $Z=N$ region. The value of Σ in an isotopic chain depends very much on the proton number. It is clear from the isotopic chains of Σ for O, Ca, Ni, Sn, Pb and $Z=114, 120$. All the considered series have their own behavior and show various trends. Generally, for lighter elements, it decreases initially to some extent and again increases monotonously. On the other hand for heavier nuclei like Pb, $Z=114$

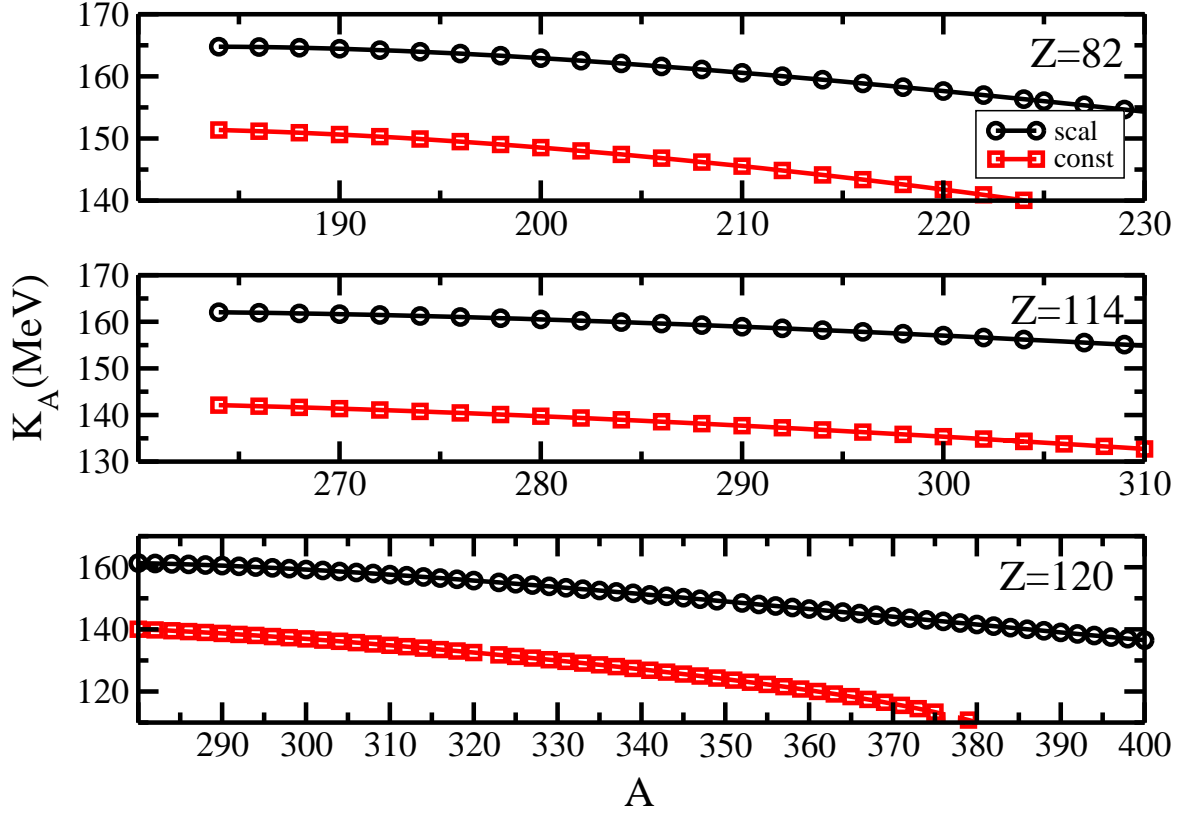
Figure 5. The compressibility modulus obtained by both scaling and constrained approaches in the isotopic series of O, Ca, Ni and Sn.



and 120 this character of Σ with mass number is somewhat different and can be seen in Fig. 4.

3.4. Compressibility modulus for finite nuclei

The nuclear matter compressibility K_∞ is a key quantity in the study of equation of state. It is the second derivative of the energy functional with respect to density at the saturation and is defined as $K_\infty = 9\rho \frac{\partial^2 \mathcal{E}}{\partial \rho^2} |_{\rho=\rho_0}$, which has a fixed value for a particular force parametrization. It is well understood that a larger K_∞ of a parameter set, gives stiff EOS and produce a massive neutron star [5]. It has also a direct relation with the asymmetry energy coefficient J of the parameter set [49]. In the limit A approaches to infinitely large, the finite nucleus can be approximated to infinite nuclear matter system ($N=Z$ for symmetry and $N \neq Z$ for asymmetry matter). Thus, it is instructive to study the nature of compressibility of finite nucleus K_A in the isotopic chain of finite nucleus. Here, we calculate the K_A as a function of mass number for the light nuclei considered in the present study (O, Ca, Ni, Sn) and then extend the calculations to Pb, Z=114 and 120 in the super heavy region. Our calculated results are shown in Figs. 5 and 6. The compressibility of finite nuclei follows same trend as the excitation energy. For light nuclei, the compressibility has small value for proton and neutron drip-lines, whereas

Figure 6. Same as Fig. 5, but for Pb, Z=114 and 120.

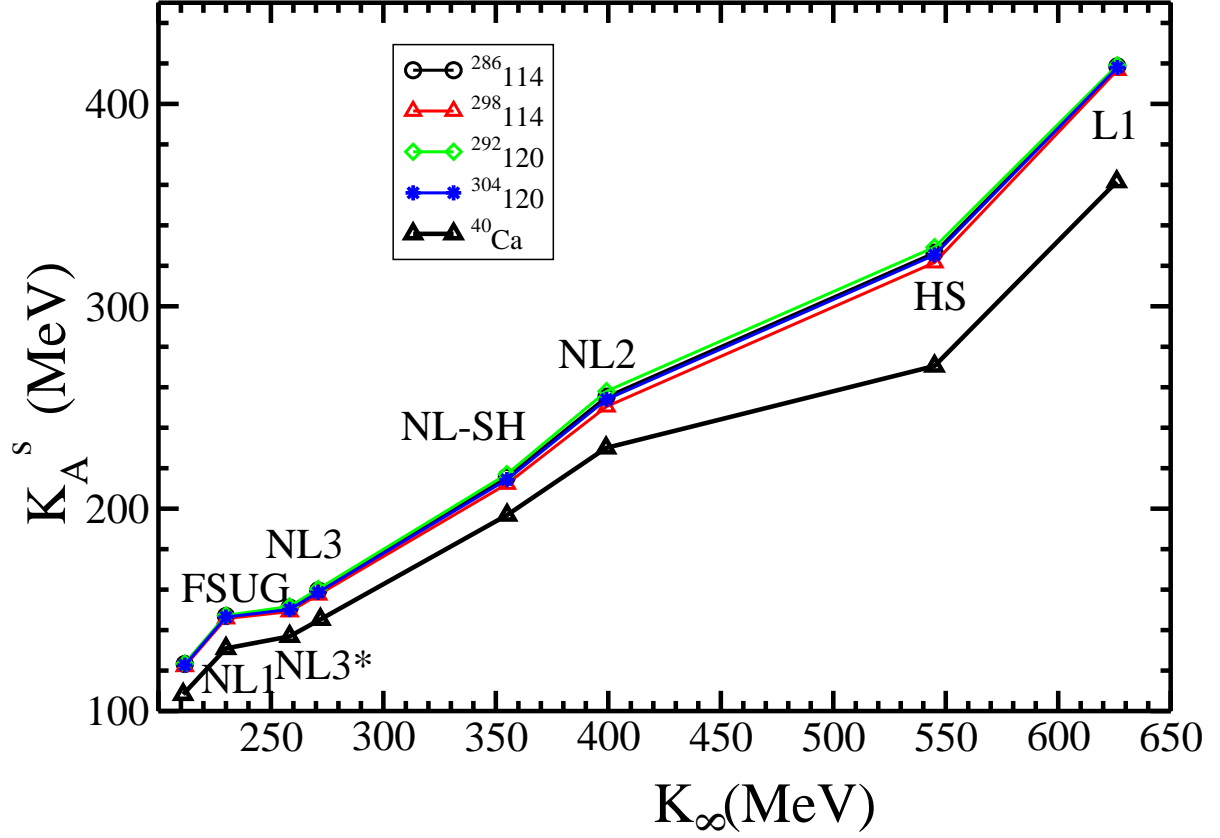
it is maximum in the neighborhood of double close combination.

It can be easily understood from Fig. 5 that, at a particular proton to neutron combination, the K_A is high, i.e., at this combination of N and Z , the nucleus is more compressible. In other word, larger the compressibility of a nucleus, it will be more compressible. Here, it is worthy to mention that the nuclear system becomes less compressibility near both the neutron and proton drip-lines. This is because of the the instability originating from the repulsive part of the nuclear force, revealing a rich neutron-proton ratio, which progressively increases with the neutron/proton number in the isotope without much affecting to the density [50]. Similar to the excitation energy, it is found that K_A obtained by scaling method is always higher than the constrained calculation. The decrease in compressibility in the drip-line regions are prominent in constrained calculation than the scaling results. From leptodermous expansion [46], we can get some basic ideas about this decreases in the vicinity of drip-lines. The expression for finite nucleus compressibility can be written as

$$K_A = K_\infty + K_{Sur}A^{-\frac{1}{3}} + K_\tau I^2 + K_{Coul}Z^2A^{-\frac{4}{3}}, \quad (27)$$

where $I = \frac{N-Z}{A}$. The coefficient K_τ is negative, so compressibility decreases with $N - Z$. For Ca chain, the compressibility obtained by scaling and constrained calculations are compared with the Hartree-Fock plus RPA

Figure 7. Compressibility for finite nuclei obtained by scaling calculation K_A^s versus nuclear matter compressibility K_∞ .



method [46] in Fig. 5. From Fig. 5, one can see that K_A evaluated by semi-classical approximation deviates from RPA results for lighter isotopes contrary to the excellent matching with the heavier mass of Ca isotopes. This is because of the exclusion of the quantal correction in the semi-classical formalism. At higher mass nuclei, this correction becomes negligible and compares to the RPA predictions. This result is depicted in Fig. 6 for Pb and super heavy chain of nuclei. Here the results show completely different trends than the lighter series. The compressibility has higher value in the vicinity of proton drip-line and decreases monotonically towards the neutron drip-line. This is because, for high Z-series, the proton drip-line appears at greater value of N in contrast to the lighter mass region. Again, the compressibility decreases with neutron number from proton to neutron drip-lines.

Finally, we would like to see the trend of K_A with nuclear matter compressibility for various force parameters and also with the size of a nucleus which can reach the infinite nuclear matter limit. For this we choose $^{286,298}_{114}$, $^{292,304}_{120}$ and ^{40}Ca as the selected candidates and shown in Fig. 7. Although, the super heavy nuclei approach the nuclear matter limit, we can not reproduce the K_∞ from K_A . This may be due to the asymmetry needed to form a bound nucleus, which is the reason for the deviation. That means, the asymmetry α of K_A and K_∞ differs

significantly (where $\alpha = \frac{N-Z}{N+Z}$), which is the main source of deviation of K_A from K_∞ . Also, this deviation arises due to the surface contribution of the finite nuclei. For a quantitative estimation, we have calculated the K_A^s for different force parameters having various K_∞ at saturation. We find almost a linear variation of K_A^s with K_∞ for the considered nuclei as shown in Fig. 7. For Ca isotopes also we find a similar nature, but smaller K_A than the super heavy nuclei.

4. Summary and Conclusions

In summary, we have calculated the isoscalar giant monopole resonance for O, Ca, Ni, Sn, Pb, Z=114 and Z=120 isotopic series starting from the proton to neutron drip-lines. The recently developed scaling approach in a relativistic mean field theory is used. A simple, but accurate constrained approximation is also performed to evaluate the isoscalar giant monopole excitation energy. From the scaling and constrained ISGMR excitation energies, we have evaluated the resonance width Σ for the whole isotopic series. This is obtained by taking the root square difference of E_x^s and E_x^c . The value of E_x^s is always higher than the constrained result E_x^c . In sum rule approach, the E_x^s can be compared with the higher and E_x^c as the lower limit of the resonance width. In general, we found an increasing trend of Σ for both lighter and super heavy region near the proton and neutron drip-lines. The magnitude of Σ is predicted to be minimum in the vicinity of N=Z or in the neighborhood of double close nucleus and it is maximum for highly asymmetry systems. In the present paper, we have also estimated the compressibility of finite nucleus. For some specific cases, the compressibility modulus is compared with the nuclear matter compressibility and found a linear variation among them. It is also concluded that the nucleus becomes less compressible with the increase of neutron or proton number in an isotopic chain. Thus the neutron-rich matter, like neutron star as well as drip-line nuclei are less compressible than the normal nuclei. In case of finite drip-line nuclei, the nucleus is incompressible, although it possess a normal density.

5. Acknowledgment:

We thank Profs. X. Viñas and M. Centelles for a careful reading of the manuscript. We also thank Mr. S. K. Singh and Mr. M. Bhuyan for discussions.

References

-
- [1] I. Tanihata, H. Hamagaki, O. Hashimoto, Y. Shida, N. Yoshikawa, K. Sugimoto, O. Yamakawa, T. Kobayashi, and N. Takahashi, Phys. Rev. Lett. **55**, 2676 (1985); A. Ozawa, T. Kobayashi, T. Suzuki, K. Yoshida, and I. Tanihata Phys. Rev. Lett. **84**, 5493 (2000); I. Tanihata, J. Phys. G: Nucl. Part. Phys. **22**, 157 (1996).
 - [2] P. G. Hansen and B. Jonson, Europhys. Lett. **4**, 409 (1989).

- [3] Yu. Ts. Oganessian et al., Phys. Rev. Lett. **104**, 142502 (2010); Yu. Ts. Oganessian et al., Phys. Rev. Lett. **83**, 3154 (1999).
- [4] K. Kumar, *Superheavy Elements*, (Adam Hilger, Bristol, 1989).
- [5] P. Arumugam, B.K. Sharma, P.K. Sahu, S.K. Patra, Tapas Sil, M. Centelles and X. Viñas, Phys. Lett. B **601**, 51 (2004).
- [6] D. H. Youngblood, H.L. Clark and Y.-W. Lui, Phys. Rev. Lett. **82**, 691 (1999).
- [7] O. Bohigas, A. Lane and J. Martorell, Phys. Rep. **51**, 267 (1979).
- [8] T. Sil, S. K. Patra, B. K. Sharma, M. Centelles and X. Viñas, Phys. Rev. C **69**, 054313 (2004); M. Bhuyan and S. K. Patra, Mod. Phys. Lett. A **27**, 1250173 (2012).
- [9] K. Rutz, J.A. Maruhn, P.-G. Reinhard and W. Greiner, Nucl. Phys. A **590**, 680 (1995).
- [10] P. Jachimowicz, M. Kowal and J. Skalski, Phys. Rev. C **83**, 054302 (2011); A. Sobczewski, F. A. Gareev and B. N. Kalinkin, Phys. Lett. **22**, 500 (1966); A. Sobczewski, Z. Patyk and S. C. Cwiok, Phys. Lett. **224**, 1 (1989); A. Sobczewski, Acta Phy. Pol. B **41**, 157 (2010); Z. Ren, Phys. Rev. C **65**, 051304(R) (2002).
- [11] M. Bhuyan, S. K. Patra and Raj K. Gupta, Phys. Rev. C **84**, 014317 (2011); S. K. Patra, M. Bhuyan, M. S. Mehta and Raj K. Gupta, Phys. Rev. C **80**, 034312 (2009); S.K. Patra, Cheng-Li Wu, C.R. Praharaaj, Raj K. Gupta, Nucl. Phys. A **651**, 117 (1999).
- [12] S. K. Patra, X. Viñas, M. Centelles and M. Del Estal, Nucl. Phys. A **703**, 240 (2002); *ibid* Phys. Lett. B **523**, 67 (2001); Chaoyuan Zhu and Xi-Jun Qiu, J. Phys. G **17**, L11 (1991).
- [13] S. K. Patra, M. Centelles, X. Viñas, and M. Del Estal, Phys. Rev. C **65**, 044304 (2002).
- [14] P. G. Reinhard et al. Z. Phys. A **323**, 13 (1986).
- [15] W. Pannert, P. Ring and J. Boguta, Phys. Rev. Lett. **59**, 2420 (1987).
- [16] G. A. Lalazissis, J. König and P. Ring, Phys. Rev. C **55**, 540 (1997).
- [17] S. K. Patra and C. R. Praharaaj, Phys. Rev. C **44**, 2552 (1991);
- [18] A. R. Bodmer, Nucl. Phys. A **526**, 703 (1991); A. R. Bodmer and C. E. Price, Nucl. Phys. A **505**, 123 (1989); Y. K. Gambhir, P. Ring, and A. Thimet, Ann. Phys. (N.Y.) **198**, 132 (1990).
- [19] K. Sumiyashi, D. Hirata, H. Toki and H. Sagawa, Nucl. Phys. A **552** 437 (1993).
- [20] Y. Sugahara and H. Toki, Nucl. Phys. A **579**, 557 (1994); S. Gmuca, J. Phys. G **17**, 1115 (1991); Z. Phys. A **342**, 387 (1992); Nucl. Phys. A **547**, 447 (1992).
- [21] C. J. Batty, E. Friedman, H. J. Gils and H. Rebel, Adv. Nucl. Phys. **19**, 1 (1989).
- [22] B. A. Brown, Phys. Rev. Lett. **85**, 5296 (2000).
- [23] B. G. Todd-Rutel and J. Piekarewicz, Phys. Rev. Lett. **95**, 122501 (2005).
- [24] F. J. Fattoyev, C. J. Horowitz, J. Piekarewicz and G. Shen, Phys. Rev. C **82**, 055803 (2010).
- [25] X. Roca-Maza, M. Centelles, X. Viñas and M. Warda, Phys. Rev. Lett. **106**, 252501 (2011).
- [26] G. A. Lalazissis, S. Karatzikos, R. Fossion, D. Pena Arteaga, A. V. Afanasjev, P. Ring, Phys. Lett. B **671**, 36 (2009).

- [27] B. D. Serot and J.D. Walecka, *Adv. Nucl. Phys.* **16**, 1 (1986).
- [28] M. Centelles, X. Viñas, M. Barranco and P. Suhuck, *Ann. Phys. (NY)* **221**, 165 (1993).
- [29] M. Centelles, X. Viñas, M. Barranco, S. Marco and R. J. Lombard, *Nucl. Phys. A* **537**, 486 (1992).
- [30] C. Speichers, E. Engle and R. M. Dreizler, *Nucl. Phys. A* **562**, 569 (1998).
- [31] M. Centelles, M. Del Estal and X. Viñas, *Nucl. Phys. A* **635**, 193 (1998).
- [32] M. Centelles, X. Viñas, M. Barranco, N. Ohtsuka, A. Faessler, Dao T. Khoa and H. Müther, *Phys. Rev. C* **47**, 1091 (1993).
- [33] M. Centelles, S. K. Patra, X Roca-Maza, B. K. Sharma, P. D. Stevenson and X. Viñas, *J. Phys. G: Nucl. Part. Phys.* **37**, 075107 (2010).
- [34] J. Boguta, A.R. Bodmer, *Nucl. Phys.* **292**, 413 (1977).
- [35] L. I. Schiff, *Phys. Rev.* **80**, 137 (1950); **83**, 239 (1951); **84**, 1 (1950).
- [36] M. Baldo, L. M. Robledo, P. Schuck and X. Viñas, *Phys. Rev.* **C87**, 064305 (2013).
- [37] X. Viñas, P. Schuck and M. Farine *J. Phys. Conf. Ser.* **321**, 012024 (2011).
- [38] T. Maruyama and T. Suzuki, *Phys. Lett. B* **219**, 43 (1989).
- [39] H. F. Boersma, R. Malfliet and O. Scholten, *Phys. Lett. B* **269**, 1 (1991).
- [40] M. V. Stoitov, P. Ring, and M. M. Sharma, *Phys. Rev. C* **50**, 1445 (1994).
- [41] M. V. Stoitsov, M. L. Cescato, P. Ring and M. M. Sharma, *J. Phys. G: Nucl. Part. Phys.* **20**, LI 49 (1994).
- [42] M. Centelles, X. Viñas, S. K. Patra, J. N. De and Tapas Sil, *Phys. Rev. C* **72**, 014304 (2005).
- [43] M. Wang, G. Audi, A. H. Wapstra, F. G. Kondev, M. MarCormick, X. Xu and B. Pfeiffer, *Chinese Physics C* **36**, 1603 (2012).
- [44] I. Angeli and K.P. Marinova, *At. Data Nucl. Data Tables*, **99**, 69 (2013).
- [45] H. A. Bethe, *Ann. Rev. Nucl. Sci.* **21**, 93 (1971).
- [46] J. P. Blaizot, *Phys. Rep.* **64**, 171 (1980).
- [47] D. H. Youngblood, Y.-W. Lui, Krishichayan, J. Button, M. R. Anders, M. L. Gorelik, M. H. Urin and S. Shlomo *Phys. Rev. C* **88**, 021301 (2013).
- [48] F. E. Bertrand, *Ann. Rev. Nucl. Part. Sc.* **26**, 456 (1976); J. Speth, A. V. Woude, *Rep. Prog. Phys.* **44**, 719 (1981); K. Goeke, J. Speth, *Ann. Rev. Nucl. Part. Sc.* **32**, 65 (1982).
- [49] M. Del Estal, M. Centelles, X. Vinas, and S. K. Patra, *Phys. Rev. C* **63**, 024314 (2001).
- [50] L. Satpathy and S. K. Patra, *J. Phys. G: Nucl. Part. Phys.* **30**, 771 (2004); S K Patra, R K Choudhury and L Satpathy, *J. Phys. G: Nucl. Part. Phys.* **37**, 085103 (2010).